

ELECTRON BEAM GENERATION AND INJECTION FROM A PYROELECTRIC CRYSTAL ARRAY

R. B. Yoder*, Z. Kabilova, and B. Saeks

Goucher College, Dept. of Physics & Astronomy, Baltimore, Maryland 21204, USA

Abstract

Novel acceleration structures (e.g. dielectric laser accelerators [DLAs] [1]) powered by lasers have the potential to greatly reduce the footprint and cost of both industrial linacs and colliders. As these devices have dimensions comparable to optical wavelengths, they require injection of a sub-micron-scale electron bunch to generate high-quality output beams, which are well beyond the capability of conventional rf photocathodes. Photoexcitation and field emission from an array of nanotips, followed by further acceleration and focusing, is a promising approach to achieving the requisite small beam sizes for successful injection. Pyroelectric crystals can provide electrostatic fields of sufficient magnitude and uniformity to enable emission and acceleration. We present an initial design for a low-energy injection module using the accelerating electrostatic fields provided by pyroelectric crystals. The approach is modeled numerically and supported by direct benchtop measurements of pyroelectric fields from a 2-crystal array.

INTRODUCTION

Novel acceleration structures, such as dielectric laser accelerators (DLAs) [1–3], continue to be a promising method for achieving high gradient optically-powered electron acceleration, greatly reducing the footprint and cost of both industrial linacs and colliders. Given the standard scaling of accelerating structures with radiation wavelength, this implies that structure dimensions must be on an optical scale, and that it will therefore require the injection or production of sub-micron-scale electron bunches for efficient monoenergetic acceleration. While this is well beyond the capability of conventional rf photocathode guns, micron-scale beams are attainable using nanotip emitters, which can be patterned or deposited on a semiconducting substrate. Field emission from nanotips has therefore been investigated as one component of an injection module for laser accelerators [4].

However, one of the challenges for optical accelerators is that their efficiency and effectiveness tend to be maximal for fully relativistic particles, when $v \sim c$. DLAs, for example, can be adapted for subrelativistic operation, but at the cost of defocusing and greatly reduced gradient [5, 6]. Injection at near-relativistic energies (several hundred keV, or $\beta = v/c \sim 0.8$) would greatly reduce this challenge.

We report here on investigation into one possible injection method, using pyroelectric crystals for field production. Pyroelectrics (e.g. crystalline ferroelectrics such as LiNbO_3 , LiTaO_3 , and BaTiO_3) are a class of materials that develop spontaneous charge polarization during heating and cooling,

producing strong surface electrostatic fields in consequence. In pyroelectric crystals, surface charges appear on the $\pm Z$ faces as long as they remain in a nonequilibrium state: negative on the $+Z$ and positive on the $-Z$ during heating, and the reverse during cooling. Because the charge attained can be very large (tens of nC per cm^2), and because relaxation to the equilibrium state via conduction through the bulk crystal is extremely slow ($\tau \sim 10^5\text{--}10^7$ sec) [7], pyroelectric crystals have been investigated as accelerators for radiation production [8, 9]. Repeated thermal cycling, perhaps combined with multiple acceleration modules, can enable continuous output.

BENCH TESTS

As a preliminary demonstration of the fields attainable from pyroelectrics, we carried out a series of bench tests on lithium niobate (LiNbO_3) crystals, in which the time-dependent temperature behavior and field production were both modeled and measured.

Charge and Temperature Measurement

The polarization of a pyroelectric crystal is proportional to its temperature change, $P_s = \gamma\Delta T$, where γ is the pyroelectric coefficient for a given material ($\gamma = 10 \text{ nC/cm}^2/\text{K}$ for LiNbO_3). The surface charge $\sigma = \pm P_s$ that appears on the $\pm Z$ faces will then dissipate over time via bulk conduction, slow charge transport across the crystal surface or its mounting, or (in air) ion transport. Combining these effects, we have a simple model for the variation of charge Q on a face over time:

$$\frac{dQ}{dt} = \gamma A \frac{dT}{dt} - \frac{1}{R_{\text{eff}} C} Q \quad (1)$$

where A is the area of a face, and R_{eff} , C are the effective resistance and capacitance between the crystal faces, respectively.

However, a further complication is that the temperature of the crystal face under test is not directly controlled, but is driven by slow thermal diffusion through the bulk from a heater on a separate face. Tests on large crystals ($>1 \text{ cm}$ in thickness) have shown that the opposite face never reaches the heater temperature [8]. Thus it becomes important to understand heat transport through LiNbO_3 crystals in order to predict and control the temperature of the field-producing face. Figure 1 shows an example of the measured temperature difference between opposite faces of one crystal, when one face is heated by a Peltier element. The temperature variation on the upper (unheated) face can be fitted to a solution of the 1-dimensional heat equation, $dT/dt = \kappa(d^2T/dx^2)$,

allowing an empirical measurement of the effective diffusivity κ of the bulk crystal.

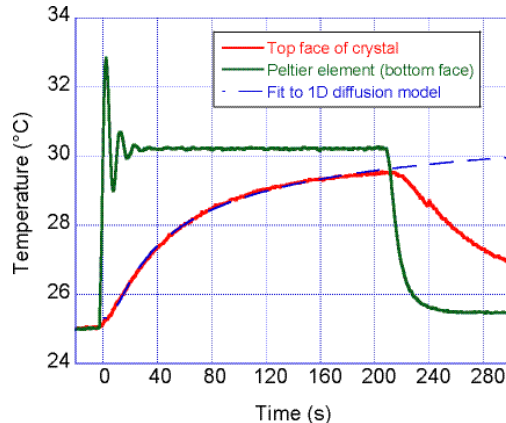


Figure 1: Sample temperature measurement, using thermistors, for a 1-cm³ LiNbO₃ crystal in vacuum, heated using a Peltier plate. The dashed curve is a fit to the heat equation, with $\kappa = 1.16 \pm 0.01$ mm²/s.

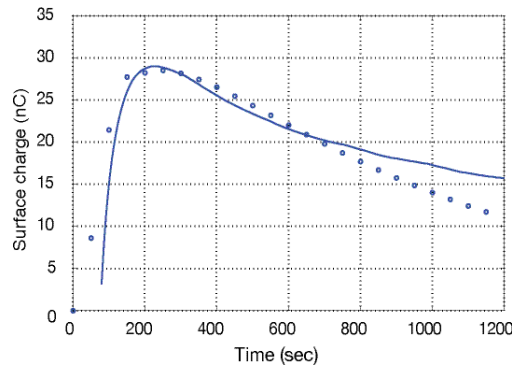


Figure 2: Measured charge (solid line) on metallized 1-cm³ LiNbO₃ crystal face in air, during steady heating to 5°C above ambient. Circles show best fit to Eq. (1), using the temperature model from Fig. 1.

The surface charge will then be a result of the changing temperature at the surface. Figure 2 shows a direct measurement of the charge produced on the metallized +Z face of a single crystal in air, using an electrometer, demonstrating that one can make reasonable estimates of the surface charge using Eq. (1) combined with knowledge of dT/dt . While the bulk resistivity of LiNbO₃ has been estimated at 10^{14} – 10^{16} Ω m [7], leading to predicted relaxation times of hours for an isolated crystal, we see an effective relaxation time of roughly 1200 sec, implying that surface or air transport is significant in this setup. We also note that the effective resistance appears to increase around 700 sec, indicating that the dominant discharge mechanism may have changed.

Field Measurement

To make a direct measurement of the fields produced by a 2-crystal array, we constructed a test stand (Fig. 3) in the modified chamber of a scanning electron microscope (SEM), in which the downward-propagating 20–30 keV SEM beam

passes through a 8-mm gap between the oppositely charged faces of two LiNbO₃ crystals. During 4–10°C heating cycles, the strong and nearly-uniform field causes deflection of the SEM beam, which can be measured by tracking its location on a 45° YAG scintillator located beneath the crystals and viewed by an external video camera. To lowest order (ideal uniform field), the deflection is proportional to field strength; a correction for nonuniform fields was determined using 2D simulation, which gives a weak quadratic dependence.

Using this setup allows measurement of the effectiveness of different heating methods. As an example, Fig. 4 shows a comparison of slower and faster heating, in which raising the heater temperature linearly over a 120-sec interval delays relaxation and results in a significantly longer “plateau” in the field than for a 60-sec interval, though the field magnitudes are comparable.

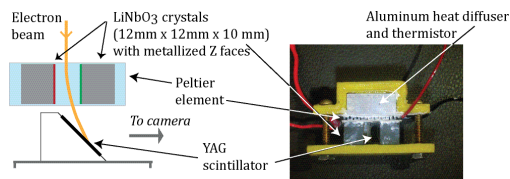


Figure 3: Test stand: side view diagram (left) and top view, photograph (right). The crystal pair is heated by a single Peltier element.

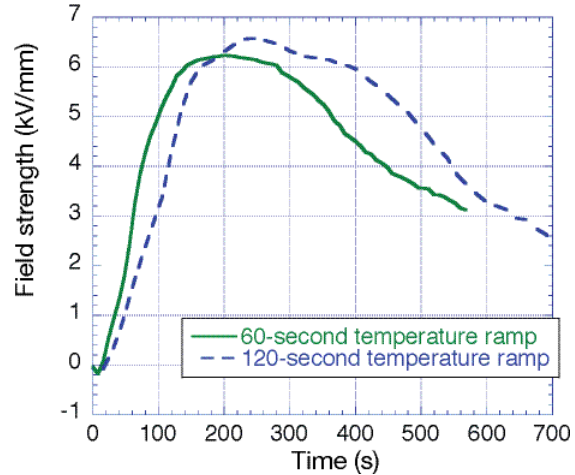


Figure 4: Field strength between oppositely-charged crystal faces for a 5° temperature increase, with heater temperature ramped linearly over 60 sec (solid line) and over 120 sec (dashed line).

A PYROELECTRIC INJECTOR

The field strengths reached in test conditions, roughly 1.2 kV/mm per degree of temperature change, are of sufficient magnitude to reach near-relativistic energies in a few cm with only moderate temperature increase, if the region of acceleration is extended through multi-staging. To assemble pyroelectric crystals into a multistage configuration that is capable of being heated and cooled, we propose to employ a narrow acceleration channel that is drilled through the

center of the crystal stack, connecting the $\pm Z$ faces, as shown in Fig. 5. When the gap between crystals is made much smaller than the crystal thicknesses along the z axis, we see significant net energy gain for electrons emitted just at the entrance of the first crystal. In the 3-crystal array results shown in Fig. 6, electrons are accelerated from zero to 305 keV in 7.3 cm (gradient 4.1 MV/m).

Of course, electrons will experience a retarding voltage if emitted into free space following the final crystal, and will require a shielding tube or other extraction mechanism to maintain this final energy. We also find that a conducting shield surrounding the crystals, but several radii away, increases the axial field.

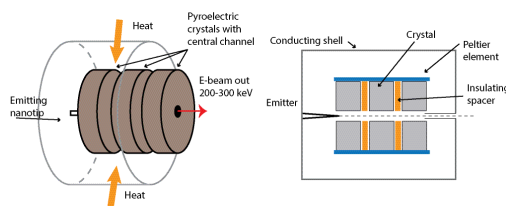


Figure 5: Concept drawing of pyroelectric stack accelerator, in different versions: cylindrically symmetric (left) and square or planar (right, in cross-section).

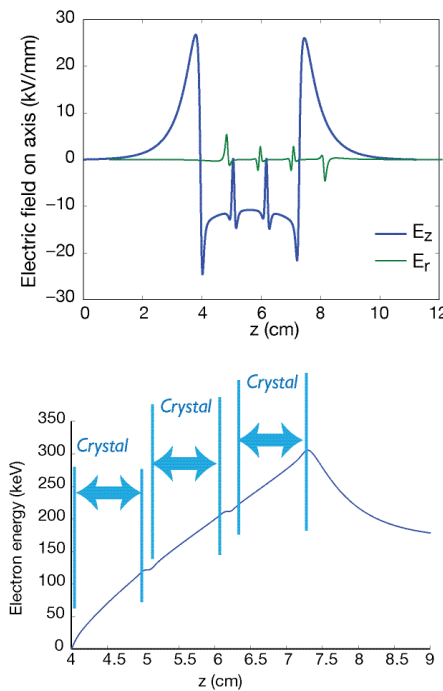


Figure 6: Top: axial electrostatic field from 2D OOPIC simulation for cylindrical 3-crystal model with 50 nC per face. Crystal radius = 6 mm, channel radius = 0.7 mm, crystal thickness = 1 cm, with conducting wall at $r = 2$ cm. Bottom: Beam energy vs. z for this example, assuming perfectly cold, zero-energy injection just inside the first crystal.

PROSPECTS AND NEXT STEPS

We have seen that pyroelectric crystal arrays can provide electrostatic fields on the order of several kV/mm, with only

a few degrees of temperature change. Once established, the fields can remain nearly constant for several minutes before the crystal begins to relax. Such a method for producing high fields without a bulky external high-voltage supply is well suited to injectors for microaccelerators in general and possible stand-alone applications in particular, in which charge production, acceleration, and radiation production all occur within a single cm-scale device. Photoexcitation of the emitter is a possible mechanism for producing a bunch train. While the device does not accelerate during the cooling part of its cycle, multiple modules in parallel could be used for continuous operation.

In future work, we will carry out emission measurements using nanotips on single crystals in test stand conditions, fully diagnosing energy and current and correlating with field production. We intend eventually to develop a proof-of-concept pyroelectric stack accelerator, demonstrating beam acceleration in a multi-crystal array after emission.

ACKNOWLEDGMENT

Support for this work was provided by the Office of the Provost, Goucher College, and the Goucher Summer Science Research Program. We thank J. Stevenson, P. Meyer, C. Gooditis, and J. Sturges for contributing to earlier stages of this work.

REFERENCES

- [1] R. J. England *et al.*, “Dielectric laser accelerators,” *Rev. Mod. Phys.*, vol. 86, p. 1337 (2014).
- [2] E. A. Peralta *et al.*, “Demonstration of electron acceleration in a laser-driven dielectric microstructure,” *Nature*, vol. 503, p. 91, 2013.
- [3] R. B. Yoder *et al.*, “First acceleration in a resonant optical-scale laser-powered structure,” in *Proc. IPAC’15*, Richmond, VA, USA, May 2015, paper WEPWA053, p. 2624.
- [4] E. R. Arab *et al.*, “Initial results on electron beam generation using pyroelectric crystals,” in *Proc. IPAC’10*, Kyoto, Japan, May 2010, paper THPD046, pp. 4384–4386.
- [5] J. McNeur *et al.*, “A tapered dielectric structure for laser acceleration at low energy,” in *Proc. IPAC’10*, Kyoto, Japan, May 2010, paper THPD047, pp. 4387–4389.
- [6] J. Breuer and P. Hommelhoff, “Laser-based acceleration of nonrelativistic electrons at a dielectric structure,” *Phys. Rev. Lett.*, vol. 111, p. 134803, 2013.
- [7] G. Rosenman *et al.*, “Electron emission from ferroelectrics,” *J. Appl. Phys.*, vol. 88, p. 6109, 2000.
- [8] T. Z. Fullem and Y. Danon, “Electrostatics of pyroelectric accelerators,” *J. Appl. Phys.*, vol. 106, p. 074101, 2009.
- [9] J. D. Brownridge and S. Shafrroth, *Appl. Phys. Lett.*, vol. 85, p. 1298, 2004.